

Celestial Walk: A Terminating Oblivious Walk for Convex Subdivisions

Wouter Kuijper
Nedap N.V.

Victor Ermolaev
Nedap N.V.

Olivier Devillers
Loria, Inria, CNRS, Université de Lorraine, France.

June 7, 2021

Abstract

We present a new oblivious walking strategy for convex subdivisions. Our walk is faster than the straight walk and more generally applicable than the visibility walk. To prove termination of our walk we use a novel monotonically decreasing distance measure.

1 Introduction

Point location in a convex subdivision is a classical problem of computational geometry for which several data structures have been designed with good complexities in the worst case [11, 4, 15]. These intricate solutions are often unused in favor of simpler algorithms based on traversal of the planar subdivisions using neighborhood relations between faces, also known as *walking algorithms* [2, 3, 9]. These walking algorithms can also be used as a building block in randomized data structures for point location [14, 6].

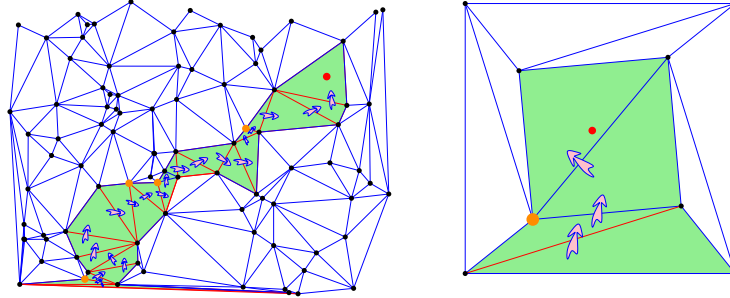


Figure 1: Celestial walk (obtuse angles marked by orange dots).

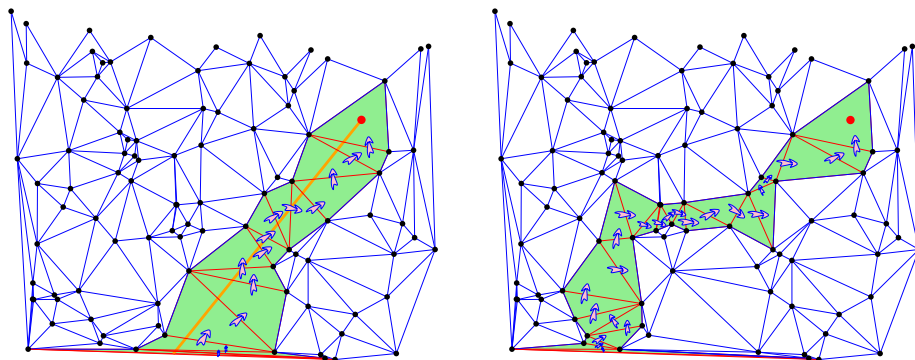


Figure 2: Straight (left) and visibility (right) walks

Amongst convex subdivisions, Delaunay triangulations received a lot of attention because of their practical importance. For Delaunay triangulations, essentially two walking strategies are used: the *straight walk* and the *visibility walk* [9]. The straight walk visits all faces crossed by a line segment between a known face and the query point, while the visibility walk goes from a face to another if the query point is on the side of the new face with respect to the supporting line of the edge common to the two faces (cf. Figure 2).

The straight walk trivially terminates in the face containing the query point and generalizes to any planar subdivision but with the inconvenience of not being oblivious: the starting face of the walk must be remembered during the whole walk.

The visibility walk is oblivious, but proving its termination requires the use of particular properties of the Delaunay triangulation, and actually the visibility walk may loop in other subdivisions [9] (cf. Figure 3).

Regarding performance, both walks may visit all triangles in the worst case and visit $O(\sqrt{n})$ triangles when the points are evenly distributed [10, 8]. From a practical point of view, the visibility walk is simpler to implement and a bit faster in practice because it uses less predicates to walk from a triangle to its

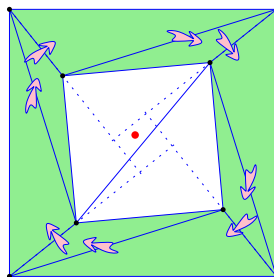


Figure 3: Visibility walk may loop

neighbor [7].

Contribution

We propose *celestial distance*¹ as a new way to measure the proximity between an edge of the subdivision and a query point. This distance measure allows to design new walking strategies and prove their termination. By design these strategies are oblivious: only the current edge of the current face determines the edges by which the walk progresses to the next face.

Our main contribution is the *celestial walk* which is a refinement of the well-known visibility walk that has the additional advantage of terminating not just on Delaunay triangulations but on arbitrary convex subdivisions. This is particularly useful for constrained and/or incremental meshing where the conditions necessary for termination of the visibility walk can be locally and/or temporarily violated.

Another important feature of the celestial walk is that, like the visibility walk, it uses only orientation predicates to navigate the mesh. In practice, checking an orientation predicate reduces to computing the sign of a second degree polynomial, the degree of such polynomial being a relevant measure of the predicate complexity [13, 1]. As a consequence, it becomes relatively straightforward to implement the celestial walk in an efficient and robust manner.

2 Pre-requisites

Let $\mathcal{G} = (V, E, F)$ be a *planar straight line graph* (PSLG) consisting of a set of vertices V , a set of half-edges E , and a set of faces F .

We abstract away the borders of \mathcal{G} by assuming that it tiles the entire real plane. At the same time we rule out dense tessellations by assuming \mathcal{G} is *locally finite* meaning the number of vertices (edges, faces) intersecting a given, bounded area is always finite.

We assume \mathcal{G} is given in half-edge representation. In particular we assume the following atomic functions [5]:

origin : $E \rightarrow V$ which maps every half-edge to its start vertex,

target : $E \rightarrow V$ which maps every half-edge to its end vertex,

edge : $F \rightarrow E$ which maps every face to some edge on its perimeter,

face : $E \rightarrow F$ which maps every half-edge to its corresponding (left-hand-side) face,

next : $E \rightarrow E$ which maps every half-edge to its successor half-edge in the counter-clockwise winding order of the face perimeter,

¹The name *celestial distance* refers to the practice of *celestial navigation* where angular distances between the celestial bodies and the horizon are used for navigation at sea.

$\text{twin} : E \rightarrow E$ which maps every half-edge to its twin half-edge running in the opposite direction, i.e.: $\text{twin}(\text{twin}(e)) = e$, $\text{origin}(e) = \text{target}(\text{twin}(e))$ and vice versa.

The *point location problem* in PSLGs can now be formulated as follows: given some goal location $p \in \mathbb{R}^2$ and an initial half-edge $e_{\text{init}} \in E$, find some goal edge $e_{\text{goal}} \in E$ such that $p \in \text{face}(e_{\text{goal}})$ using only $\text{next}(\cdot)$ and $\text{twin}(\cdot)$ to get from one half-edge to the next, i.e.: there must exist a finite path $e_{\text{init}} = e_0 \dots e_n = e_{\text{goal}}$ such that for all $0 < i \leq n$ it holds $e_i = \text{next}(e_{i-1})$ or $e_i = \text{twin}(e_{i-1})$.

3 Celestial Distance

One problem that we encounter when we try to use Euclidean distance as a measure of progress for a walking algorithm is the fact that Euclidean distance is not always strictly decreasing for every step in the walk. The latter means that it is not possible to prove termination using Euclidean distance alone. For this reason we define the following augmented distance measure on (half-)edges.

For a given point $p \in \mathbb{R}^2$ and a half-edge $e \in E$ we define the *celestial distance* of e to p as a pair $\text{cd}(e, p) = [d, \alpha]$ where d is the length of the line segment from p to the closest point on e and α is the wide angle ($\alpha \geq \frac{\pi}{2}$) between e and this line segment or 0 in case $d = 0$. We now define a lexicographic order on celestial distances as follows:

$$[d, \alpha] < [d', \alpha'] \text{ iff } d < d' \vee (d = d' \wedge \alpha < \alpha')$$

We illustrate this new distance measure in Figure 4. The figure shows a convex face and the resulting partition of the plane obtained by grouping together points based on their closest edge. This leads to two superimposed Voronoi partitions: one based on classical Euclidean distance and one based on celestial distance. The partition based on celestial distance is a proper refinement of the partition based on Euclidean distance in the sense that points which were ambiguous under Euclidean distance are now partitionable under celestial distance. Note that the points in the corner-cones radiating outward from the vertices are all ambiguous under Euclidean distance (since their closest point on the polygon is the corner vertex which is shared by two edges) yet under celestial distance they can be further partitioned. In particular, for the partition based on celestial distance the ambiguous corner-cones are split according to the angular bisectors.

4 Abstract Walk

With all the pre-requisites and our celestial distance measure in place we are in a position to present the walking algorithm properly. We first present an abstract version of the algorithm and give a correctness proof for this abstract version.

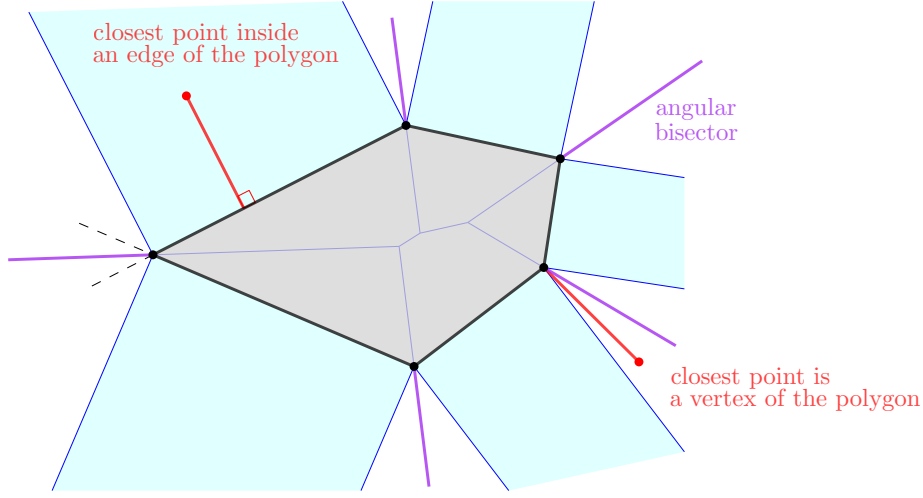


Figure 4: Voronoi diagrams of a polygon. In blue the segment Voronoi diagram of the open edges and the vertices, in purple the celestial Voronoi diagram of the edges.

In the next section, we will give an efficient, concrete instantiation of this abstract version where the computation of the celestial distances will be completely implicit. However, the correctness of the final version will rest on the correctness proof of the abstract version as given in this section.

Algorithm 1 Abstract Walk

```

1: if  $p$  strictly right of  $e$  then
2:    $e \leftarrow \text{twin}(e)$ 
3: end if
4:  $E' \leftarrow \{e\}$ 
5: while  $E' \neq \emptyset$  do
6:    $e \leftarrow \text{select}(E')$ 
7:    $E' \leftarrow \{\text{twin}(e') \mid e' \in \text{face}(e) \wedge \text{cd}(e', p) < \text{cd}(e, p) \wedge p \text{ strictly right of } e'\}$ 
8: end while
9: return  $\text{face}(e)$ 

```

The algorithm is rather simple: given a starting edge e and a query point p to the left of e , we select an edge of the $\text{face}(e)$ that improves the distance to p . The abstract walk is formalized in Algorithm 1.

In lines 1-3 we bootstrap the invariant that the query point is always to the left of the current edge. In line 4 we bootstrap the current set of successor candidates. In line 5 we enter the main loop. The loop invariant ensures that the loop will terminate as soon as there are no more suitable successor edges

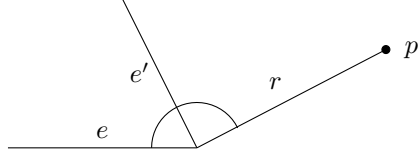


Figure 5: Illustration for limit case of Theorem 1.

that have lower celestial distance to the query point. In the proof below we will see how this condition is sufficient to ensure that, at termination, it holds $p \in \text{face}(e)$. In line 6 we non-deterministically select one of the candidate successor edges. In line 7 we compute the next set of candidate successor edges which are all edges on the current face perimeter that have the query point on the right and have smaller celestial distance to the query point than the current edge.

Theorem 1. *For any planar subdivision, starting edge, and query point Algorithm 1 terminates with $p \in \text{face}(e)$.*

Proof. For termination note that, due to local finiteness of the mesh, and monotonicity of our distance measure, an infinitely descending chain of celestial distances is ruled out. It remains to prove that after termination it holds $p \in \text{face}(e)$. For this it would suffice to show that for a half-edge e and goal location p such that p is to the left-of e but not in $\text{face}(e)$ there always exists another e' in the perimeter of $\text{face}(e)$ such that p is strictly on the right of e' and $\text{cd}(e', p) < \text{cd}(e, p)$. So let e_p be the point on e closest to p and let r be the ray from p to e_p . We make a case distinction on r . First assume that r intersects the interior of $\text{face}(e)$. In this case it must hold that r intersects the boundary of $\text{face}(e)$ at least one more time in another edge that is closer to p than the current edge for the Euclidean distance, and thus for our celestial distance (otherwise p would lie in the current face). Next assume that r does not intersect the interior of $\text{face}(e)$. In this case it must hold that $e_p = \text{origin}(e)$ or $e_p = \text{target}(e)$. Assume, w.l.o.g., that $e_p = \text{target}(e)$. In this case we claim that it holds that $e' = \text{next}(e)$ has strictly smaller celestial distance to p . Assume, w.l.o.g., that e' provides no improvement over e w.r.t. Euclidean distance to p . It then immediately follows that the closest point on e' to p must be the only point that e and e' share which, by assumption, is $e_p = \text{target}(e) = \text{origin}(e')$. Since r does not intersect the boundary of $\text{face}(e)$ in any point other than e_p it must hold that e' is in-between e and r (cf. Figure 5). Now it holds that: $\text{wideangle}(e, r) = \text{angle}(e, e') + \text{wideangle}(e', r)$ which implies $\text{wideangle}(e', r) < \text{wideangle}(e, r)$. This establishes $\text{cd}(e', p) < \text{cd}(e, p)$ and we conclude the algorithm would progress to $\text{twin}(e')$. \square

5 Celestial Walk

In the previous section, the successor of an edge in the walk can be the twin of any edge of the current face with a smaller distance to the query point. In this section, we explain a way to actually select such an edge using only orientation checks.

The main problems that we are solving in this section are the facts that Algorithm 1 is non-deterministic and relies on the explicit computation of celestial distances. Both these properties make it less immediately applicable. In this section we therefore develop a derived algorithm that works for *convex* PSLGs. As we shall see, the additional assumption of convexity allows us a significantly more efficient walk.

So let us first consider the problem of determining a successor edge that has lower celestial distance than our current edge without having to explicitly compute these distances.

As an example of a convex face consider once more Figure 4. If we assume the query point is outside the face this leaves two possibilities. First, the query point may be located inside one of the orthogonal slabs (indicated in blue in Figure 4) which means the closest point coincides with the orthogonal projection of the query point on the edge. Second, the query point may be located in one of the intermediate corner-cones separating the orthogonal slabs which means the closest point coincides with the corner vertex.

The latter argument gives us a basic refinement of Algorithm 1 for the convex case: check if the query point is in one of the orthogonal slabs, if so, pick the corresponding edge, else the query point must be inside some corner-cone in-between two orthogonal slabs, in this case we can pick either edge (unless one of them is our current edge in which case we are forced to pick the other alternative in order to make progress).

To do even better we can resolve the remaining non-determinism by using the angle as a tie-breaker to determine which of the two candidate edges is best (i.e.: which edge is most favorably oriented towards the query point). Theoretically the best tie breaker is the angular bisector (indicated in purple in Figure 4). The only problem is that the explicit computation and representation of the exact angular bisector is at least as hard as the explicit computation and representation of celestial distances.

Fortunately we can avoid the explicit computation of angular bisectors as well. In particular we make the following case distinction. If the corner vertex is *not obtuse* (more precisely the face has an acute or right internal angle at that corner vertex) it holds that the extensions of both edges lie inside the corner-cone (i.e.: the leftmost corner in Figure 4). This means that we may use either edge itself as a crude approximation to the angular bisector (this is precisely what the visibility walk does in *all* cases). On the other hand, if the corner vertex is *obtuse* it holds that the normal to the base of the triangle spanned by the two candidate edges forms a suitable approximation to the angular bisector (because it lies properly inside the corner-cone). In Figure 6 we illustrate this construction. Note that, in the limit, as the internal angle

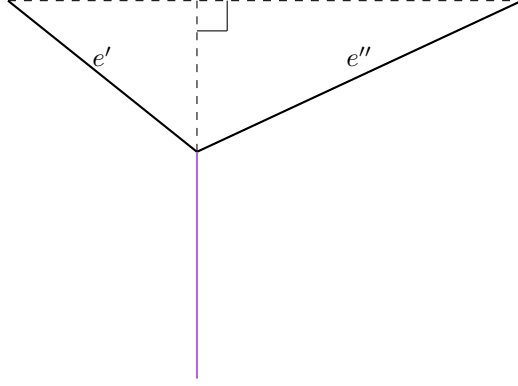


Figure 6: Construction for approximating angular bisector.

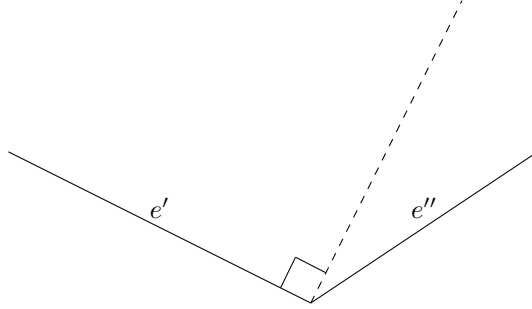


Figure 7: Reducing obtuseness check to orientation check.

approaches 180 degrees, or, alternatively, the ratio between the lengths of the two edges approaches 1, the base normal converges to the exact angular bisector.

The latter considerations lead us to define $\text{approx_bisector}(e', e'')$ for some pair of consecutive edges e', e'' such that $e'' = \text{next}(e')$ and $\text{angle}(e', e'')$ is obtuse. In particular, we let $\text{approx_bisector}(e', e'')$ denote the line from $\text{target}(e')$ — which is equal by definition to $\text{origin}(e'')$ — in the direction orthogonal to, and to the right of, the internal baseline segment that connects $\text{origin}(e')$ and $\text{target}(e'')$. For an illustration of this construction cf. Figure 6. We also define $\text{obtuse}(e', e'')$ as a predicate that is true iff $\text{target}(e'')$ is strictly right of the line from $\text{target}(e')$ — which we assumed is equal to $\text{origin}(e'')$ — in the direction orthogonal to, and to the left of, e' . For an illustration of this construction cf. Figure 7. With these additional definitions Algorithm 2 formalizes the celestial walk.

In lines 1-3 we bootstrap the invariant that the query point is always to the left of the current edge. In line 4 we initialize a perimeter edge variable used for iterating over the outline of the current face. In line 5 we enter the outer loop. As can be seen by inspecting the code-paths inside the loop body, the

Algorithm 2 Celestial Walk

```
1: if  $p$  strictly right of  $e$  then
2:    $e \leftarrow \text{twin}(e)$ 
3: end if
4:  $e' \leftarrow \text{next}(e)$ 
5: while  $e \neq e'$  do
6:   if  $p$  strictly right of  $e'$  then
7:      $e'' \leftarrow \text{next}(e')$ 
8:     while obtuse( $e', e''$ ) and  $p$  left of approx_bisector( $e', e''$ ) do
9:        $e', e'' \leftarrow e'', \text{next}(e'')$ 
10:    end while
11:     $e \leftarrow \text{twin}(e')$ 
12:     $e' \leftarrow \text{next}(e)$ 
13:   else
14:      $e' \leftarrow \text{next}(e')$ 
15:   end if
16: end while
17: return face( $e$ )
```

loop invariant ensures that the loop will terminate iff the query point is inside the current face. In line 6 we check if the query point lies strictly to the right of the perimeter edge. If this is the case we know, due to the face convexity, that the query point is outside the face. From that moment on the only goal is to find an edge that allows us to walk to a neighboring face. Therefore, in line 7 we introduce a second perimeter edge variable that will be used to iterate over *pairs* (e', e'') of consecutive edges rather than singletons. In line 8 we state the negation of the condition that we are looking for: either the internal angle of the face is acute² or, otherwise, the query point falls strictly to the right of the approximate bisector. In line 9 we shift the pair of edges along the face perimeter until said condition is reached. In line 11 we have exited the inner loop so we know that e' contains the edge that is “sufficiently closest” to the query point for us to continue the walk to the neighboring face. Hence we reassign e and e' and drop back into the outer loop as though we would have restarted the algorithm on this new edge.

The latter can be seen as a form of tail-recursion. Indeed, a recursive formulation is trivially possible by transforming the entire procedure into a function and substituting a recursive call at line 12. We have not opted for the recursive formulation because it would be slightly less efficient. The efficiency loss would be due to the bootstrapping check in lines 1-3 which, in the recursion, would be superfluous.

²Note that the obtuseness check in line 8 can potentially be memorized by the mesh at the expense of one bit per half-edge.

6 Conclusion

We have shown how our celestial distance measure allows to design novel walking strategies. In particular we improved the applicability of the popular visibility walk by refining it into what we call the celestial walk. Our walk is almost as simple to implement yet is guaranteed to terminate on arbitrary convex subdivisions.

If we assume that all obtuseness checks are pre-computed or memoized (at the expense of 1 or 2 bits per half-edge respectively) we can make the following observations w.r.t. the expected complexity of our walk.

The worst case for our walk materializes when all angles in the mesh are obtuse, i.e. in a regular hexagonal mesh, in this case we require 2 orientation tests per visited half-edge (the same number as the straight walk).

For triangulations a simple counting argument proves that there is at most a fraction of $\frac{1}{3}$ of obtuse angles. This gives us a worst case rough estimate of $\frac{4}{3}$ orientation tests per visited half-edge (better than the straight walk and only slightly worse than the visibility walk). In practice, we expect better performance since the fraction of obtuse angles will be much less than $\frac{1}{3}$ in triangulations that exhibit some regularity.

For meshes that are guaranteed to be triangular, minor optimizations are possible by unrolling the loops of the general algorithm. Furthermore, it is a good heuristic to minimize the number of visited triangles by alternating clockwise and counterclockwise winding order in order to balance out the systematic errors in approximating the angular bisectors.

Future Work

An obvious next question to consider is whether the walk can be generalized to 3 dimensions. We have some reason to believe this is the case.

In 2D as we progress according to the celestial walk we either move forward in the direction of the query point or *orient* ourselves towards it. Similarly, in 3 dimensions we expect to either progress in Euclidian sense or *roll* in the direction of the query point. This intuition leads to developing a suitable non-increasing distance measure quantifying this relationship. In particular to the walking problem in tetrahedralization we find that a combination of Euclidian distance as the first progression criterion and two successive angles are sufficient to guarantee the progress towards the tetrahedron containing the query point [12].

Finally, we would also be interested in obtaining experimental results regarding the trade-off that exists between steering (i.e.: choosing a next edge that is favorably oriented to the query point) and driving (i.e.: choosing a next edge *quickly* based on easily computed criteria).

References

- [1] J.-D. Boissonnat and F. P. Preparata. Robust plane sweep for intersecting segments. *SIAM Journal on Computing*, 29(5):1401–1421, 2000.
- [2] P. Bose, A. Brodnik, S. Carlsson, E. D. Demaine, R. Fleischer, A. López-Ortiz, P. Morin, and J. Ian Munro. Online routing in convex subdivisions. *International Journal of Computational Geometry & Applications*, 12(04):283–295, 2002.
- [3] P. Bose and P. Morin. Online routing in triangulations. *SIAM journal on computing*, 33(4):937–951, 2004.
- [4] B. Chazelle and L. J. Guibas. Fractional cascading: I. a data structuring technique. *Algorithmica*, 1(1):133–162, 1986.
- [5] M. de Berg, M. van Kreveld, M. Overmars, and O. Schwarzkopf. *Computational Geometry: Algorithms and Applications*. Springer-Verlag, Berlin, 1997.
- [6] O. Devillers. The Delaunay Hierarchy. *International Journal of Foundations of Computer Science*, 13:163–180, 2002.
- [7] O. Devillers. Delaunay triangulations, theory vs practice. In *EuroCG, 28th European Workshop on Computational Geometry*, Assisi, Italy, 2012.
- [8] O. Devillers and R. Hemsley. The worst visibility walk in a random Delaunay triangulation is $O(\sqrt{n})$. *Journal of Computational Geometry*, 7(1):332–359, 2016.
- [9] O. Devillers, S. Pion, and M. Teillaud. Walking in a Triangulation. *International Journal of Foundations of Computer Science*, 13:181–199, 2002.
- [10] L. Devroye, C. Lemaire, and J.-M. Moreau. Expected time analysis for delaunay point location. *Computational geometry*, 29(2):61–89, 2004.
- [11] D. Kirkpatrick. Optimal search in planar subdivisions. *SIAM Journal on Computing*, 12(1):28–35, 1983.
- [12] W. Kuijper, V. Ermolaev, and H. Berntsen. Zig-zagging in a triangulation. *arXiv preprint arXiv:1705.03950*, 2017.
- [13] G. Liotta, F. P. Preparata, and R. Tamassia. Robust proximity queries: An illustration of degree-driven algorithm design. *SIAM Journal on Computing*, 28(3):864–889, 1998.
- [14] E. P. Mücke, I. Saias, and B. Zhu. Fast randomized point location without preprocessing in two-and three-dimensional Delaunay triangulations. *Computational Geometry*, 12(1-2):63–83, 1999.
- [15] F. P. Preparata. Planar point location revisited. *International Journal of Foundations of Computer Science*, 1(01):71–86, 1990.